

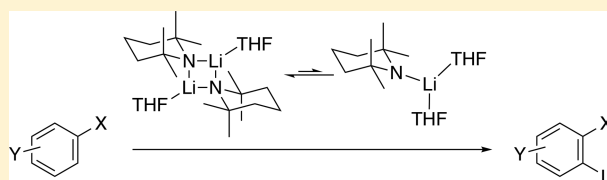
# Case for Lithium Tetramethylpiperidide-Mediated Ortholithiations: Reactivity and Mechanisms

Kyle A. Mack and David B. Collum\*<sup>1</sup>

Department of Chemistry and Chemical Biology Baker Laboratory, Cornell University, Ithaca, New York 14853-1301, United States

**S** Supporting Information

**ABSTRACT:** Rate and mechanistic studies of ortholithiations by lithium 2,2,6,6-tetramethylpiperidide focus on four arenes: 1,4-bis(trifluoromethyl)benzene, 1,3-bis(trifluoromethyl)benzene, 1,3-dimethoxybenzene, and 4,4-dimethyl-2-phenyl-2-oxazoline. Metalations occur via substrate-dependent combinations of monosolvated monomer, disolvated monomer, and tetrasolvated dimer (triple ions). Density functional theory computational studies augment the experimental data. We discuss the challenges presented by shifting dimer–monomer proportions in determining the observable reaction orders and our mathematical treatment of such shifting in reactant structure.



## INTRODUCTION

Few transformations are more important than functionalizations of C–H bonds on aromatic and heteroaromatic rings.<sup>1</sup> Traditional electrophilic aromatic substitutions are limited to electron-rich arenes, have marginal regioselectivities, and can generate noxious waste streams when used on scale.<sup>2</sup> Emergent efforts to achieve catalytic transition-metal-mediated C–H activations are making great strides but remain in the early to mid-developmental stages.<sup>3</sup> Ortholithiations with subsequent trapping by electrophiles are not without limitations but generally offer high reactivities of organolithium bases and exceptional regiocontrol.<sup>4,5</sup>

The choice of base for orthometalations has chemical, economic, and safety consequences. Lithium diisopropylamide (LDA) is ideal for relatively acidic, multifunctional arenes.<sup>5</sup> Less reactive arenes are most often metalated using *n*- or *sec*-butyllithium facilitated by a variety of accelerants such as tetrahydrofuran (THF) or *N,N,N',N'*-tetramethylethylenediamine. There are, however, some large disparities separating LDA and alkyllithiums: the high basicity and reactivity offered by alkyllithiums is offset by functional group incompatibilities. Note that casual mentions of basicity and reactivity can connote kinetic or thermodynamic effects depending on context. Does a base observably metalate (thermodynamic) and, if so, how fast (kinetic)?

Nestled between LDA and alkyllithiums lies lithium 2,2,6,6-tetramethylpiperidide (LiTMP).<sup>6</sup> This base has been used for many ortholithiations, of course, but we sense that many practitioners are unaware of its advantages. LiTMP is not simply a more expensive equivalent of LDA. LiTMP-mediated metalations have a greater driving force<sup>7,8</sup> and disproportionately higher metalation rates, both of which may stem from high steric demands that inhibit stabilizing aggregation: a form of ground-state destabilization. The high steric demands also amplify sterically dictated regiocontrol, and the hindered 2,2,6,6-tetramethylpiperidine (TMPH) byproduct precludes

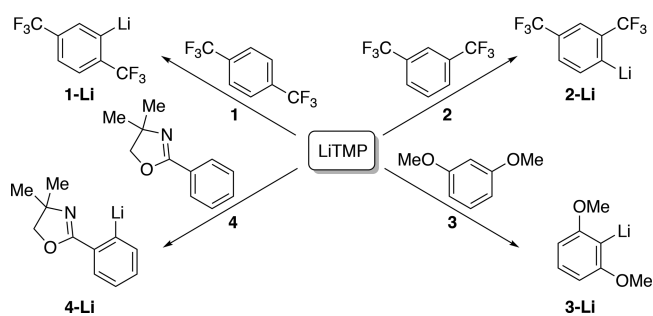
regiochemical equilibrations that are readily mediated by *i*-Pr<sub>2</sub>NH.<sup>9–11</sup> The higher cost of TMPH is also a red herring. TMPH is significantly more expensive than *i*-Pr<sub>2</sub>NH, but current prices are markedly lower in bulk and should be susceptible to further downward pressure given that TMPH is prepared from acetone, ammonia, hydrazine, and KOH.<sup>12</sup>

This paper describes our progress beyond the above analysis through the probing of a combination of selectivities and mechanisms of LiTMP-mediated ortholithiations. Although the selectivities are largely founded in prior art,<sup>13</sup> only one detailed rate and mechanistic study of an LiTMP-mediated reaction, an epoxide elimination, has been reported.<sup>14,15</sup> We surveyed more than 40 arene metalations and selected arenes 1–4 (Scheme 1) for detailed study.

## RESULTS

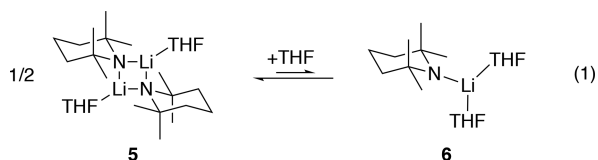
Spectroscopic studies have shown that LiTMP is a 10:1 mixture of dimer 5 and monomer 6 in neat THF and >99:1 dimer at <1.3 M THF–hexane (eq 1).<sup>16</sup> The dimer–monomer solvation

**Scheme 1. Lithium 2,2,6,6-Tetramethylpiperidide-Mediated Metalations of Arenes**



Received: January 16, 2018

Published: March 28, 2018



states were first studied with semiempirical calculations<sup>17</sup> that were later augmented with density functional theory (DFT) computations.<sup>18,19</sup> To simplify the presentation, we use the following shorthand: A = LiTMP subunit; S = THF; ArH = arene; ArLi = aryllithium. For example,  $A_2S_2$  is a disolvated dimer and  $[A_2S_2(ArH)]^\ddagger$  is the corresponding disolvated-dimer-based transition structure.

**Kinetics: General Protocol.**<sup>20</sup> LiTMP was held in excess at standard concentrations (0.025–0.25 M). THF was also used in high but variable concentrations (2.6–12.2 M) with hexane as a cosolvent. Arenes were the limiting reagents (0.0025–0.010 M). Metalation rates were monitored using in situ IR spectroscopy by following the loss of strong arene absorbances in the range of 1323–1655  $\text{cm}^{-1}$ . The time-dependent decays fit the first-order function  $f(x) = ae^{-bx}$  such that  $b$  corresponds to the pseudo-first-order rate constant,  $k_{\text{obsd}}$ . Values of  $k_{\text{obsd}}$  were shown to be independent of initial arene concentration as required for a first-order dependence. On occasion, initial rates were used if the LiTMP/ArH proportions deviated from pseudo-first order. All metalations displayed large isotope effects ( $k_{\text{obsd(H)}}/k_{\text{obsd(D)}} = 23\text{--}40$ ), which confirmed rate-limiting proton transfers. Large isotope effects in orthometalations, which suggests tunneling, are common.<sup>20a</sup> A standard control experiment excluded the intervention of autocatalysis.<sup>20b</sup> After a first-order decay, the baseline was re-established, and a second aliquot of arene was injected; the two rate constants were indistinguishable.

The orders in THF were determined by monitoring  $k_{\text{obsd}}$  versus THF concentration using hexane as the cosolvent. Similarly, plots of  $k_{\text{obsd}}$  versus LiTMP concentration afforded orders in LiTMP. The LiTMP dimer–monomer equilibrium in eq 1 presents added mathematical complexity to attaining rigorous fitting of THF and LiTMP concentration dependencies. We routinely cite orders stemming from fits to a simple power function ( $y = ax^n$ ). The fits shown graphically, by contrast, are more rigorous and complex, as described below.

To account for the shift in ground state from dimer ( $A_2S_2$ ) to monomer ( $AS_2$ ), we must solve for the monomer and dimer concentrations as a function of the equilibrium constant ( $K_{\text{eq}}$ ), total base concentration ( $[A_{\text{total}}]$ ), and total solvent concentration ( $[S]$ ). Solving the system of two eqs (eq 2 and 3) provides two sets of roots. We chose the sets corresponding to real, positive concentrations.

$$K_{\text{eq}} = \frac{[AS_2]^2}{[A_2S_2][S]^2} \quad (2)$$

$$[A_{\text{total}}] = 2[A_2S_2] + [AS_2] \quad (3)$$

$$[A_2S_2] = \frac{1}{8}(4[A_{\text{total}}] + K_{\text{eq}}[S]^2 - \sqrt{K_{\text{eq}}[S] \sqrt{8[A_{\text{total}}] + K_{\text{eq}}[S]^2}}) \quad (4)$$

The choice of species ( $A_2S_2$  versus  $AS_2$ ) for writing rate expressions is arbitrary:  $A_2S_2$  was chosen because of its dominance across the accessible THF concentration range

(vide infra). Equation 4 describes the concentration of  $A_2S_2$ . In the Discussion, we return to the challenges posed by two or more observable reactants with concentrations that vary with reaction conditions.

**1,4-bis-(trifluoromethyl)benzene (1).** A plot of  $k_{\text{obsd}}$  versus THF concentration (Figure 1) for the metalation of 1

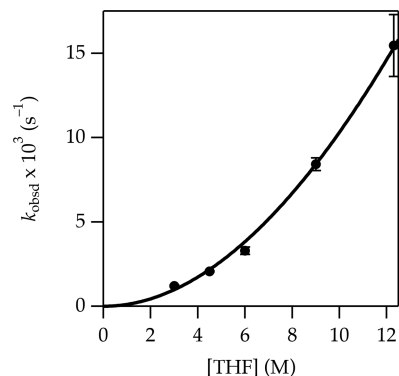


**Figure 1.** Plot of  $k_{\text{obsd}}$  vs tetrahydrofuran (THF) concentration for the metalation of 1 (0.010 M) at  $-78^\circ\text{C}$  measured with IR spectroscopy (1323  $\text{cm}^{-1}$ ). The curve depicts an unweighted least-squares fit to eq 5 that accounts for the shifting dimer–monomer mixtures described by eq 4. A simple fit to  $y = ax^n$  affords  $a = 0.10 \pm 0.02$ ,  $n = 2.02 \pm 0.07$ .

to form 1-Li shows a clean second-order dependence,  $n = 2.02 \pm 0.07$  when fit to a simple power function, although a rigorous fit is more complex (vide infra). A plot of  $k_{\text{obsd}}$  versus LiTMP concentration at a 6.0 M THF concentration (Figure 2) shows

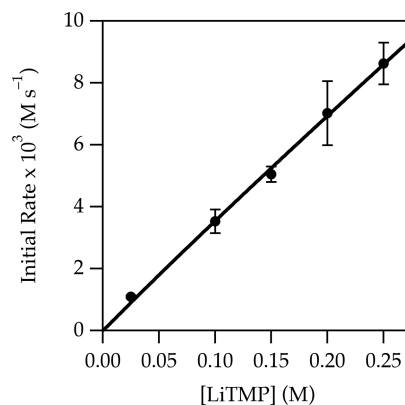
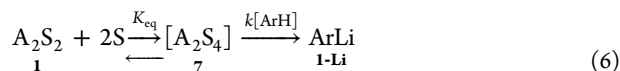


**Figure 2.** Plot of initial rate vs lithium 2,2,6,6-tetramethylpiperidide (LiTMP) concentration for the metalation of 1 (0.010 M) in 6.0 M THF/hexane at  $-78^\circ\text{C}$  measured with IR spectroscopy (1323  $\text{cm}^{-1}$ ). The curve depicts an unweighted least-squares fit to eq 5 that accounts for the shifting dimer–monomer mixtures described by eq 4. A simple fit to  $y = ax^n$  affords  $a = 33.07 \pm 2.19$ ,  $n = 0.97 \pm 0.04$ .

an approximate first-order dependence. (Origins of the slight downward curvature are discussed in detail below.) When these results are taken together, the idealized rate law<sup>21</sup> in eq 5 is consistent with the generic mechanism shown in eq 6.

$$d[\text{ArLi}]/dt = k[\text{ArH}]^1[\text{S}]^2[\text{A}_2\text{S}_2]^1 \quad (5)$$



Owing to the severe steric hindrance of an  $A_2S_4$  cyclic dimer<sup>15–18</sup> as a reactant or a transition structure, the rate data

implicate triple ions.<sup>22</sup> Such LiTMP-derived triple ions have been structurally characterized<sup>23</sup> and studied computationally.<sup>17</sup>

**1,3-bis-(trifluoromethyl)benzene (2).** The metalation of **2** at  $-78$  °C affords exclusively the 4-lithiated product **2-Li** as shown by deuteration. Fitting the THF dependence to a simple power function shows an intermediate order of  $1.50 \pm 0.04$  (Figure 3), which suggests at least two mechanisms at play.

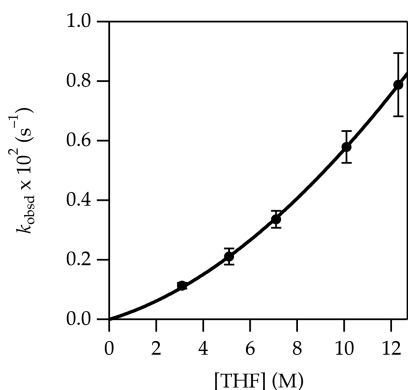


**Figure 3.** Plot of  $k_{\text{obsd}}$  vs THF concentration for the metalation of **2** (0.0025 M) at  $-78$  °C measured with IR spectroscopy ( $1356\text{ cm}^{-1}$ ). The curve depicts an unweighted least-squares fit to eq 7 that accounts for the shifting dimer–monomer mixtures described by eq 4. A simple fit to  $y = ax^n$  affords  $a = 0.018 \pm 0.002$ ,  $n = 1.50 \pm 0.04$ .

Similarly, the measured LiTMP order fit to a power function is  $0.76 \pm 0.04$  (Figure 4), which attests to competing monomer-

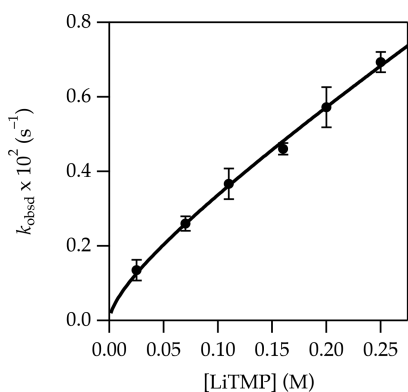
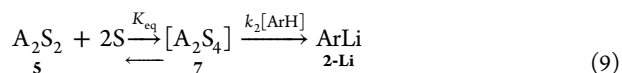
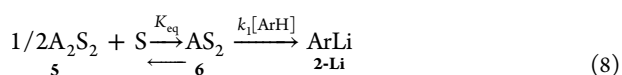


**Figure 4.** Plot of  $k_{\text{obsd}}$  vs LiTMP concentration for the metalation of **2** (0.0025 M) in 6.0 M THF/hexane at  $-78$  °C measured with IR spectroscopy ( $1356\text{ cm}^{-1}$ ). The curve depicts an unweighted least-squares fit to eq 7 that accounts for the shifting dimer–monomer mixtures described by eq 4. A simple fit to  $y = ax^n$  affords  $a = 1.9 \pm 0.1$ ,  $n = 0.76 \pm 0.04$ .

and dimer-based metalations. The fits in Figures 3 and 4 are consistent with the idealized rate law in eq 7 and the mechanisms shown in eqs 8 and 9.<sup>24</sup>

$$\frac{d[\text{ArLi}]}{dt} = k_1[\text{ArH}]^1[\text{S}]^1[\text{A}_2\text{S}_2]^{1/2} + k_2[\text{ArH}]^1[\text{S}]^2[\text{A}_2\text{S}_2]^1 \quad (7)$$



**1,3-bis-(methoxy)benzene (3).** The metalation of **3** at  $-40$  °C to form **3-Li** shows a clean first-order THF dependence (Figure 5) and half-order LiTMP dependence

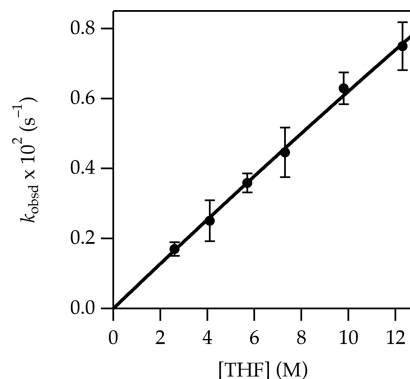


**Figure 5.** Plot of  $k_{\text{obsd}}$  vs free THF concentration for the metalation of **3** (0.0025 M) at  $-40$  °C measured with IR spectroscopy ( $1496\text{ cm}^{-1}$ ). The curve depicts an unweighted least-squares fit to eq 10 that accounts for the shifting dimer–monomer mixtures described by eq 4. A simple fit to  $y = ax^n$  affords  $a = 0.065 \pm 0.005$ ,  $n = 0.98 \pm 0.03$ .

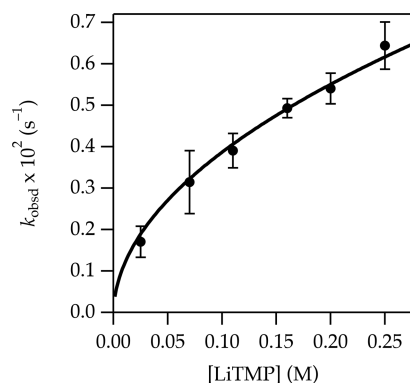
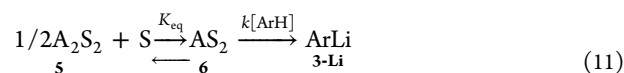


**Figure 6.** Plot of  $k_{\text{obsd}}$  vs LiTMP concentration for the metalation of **3** (0.0025 M) in 6.0 M THF/hexane at  $-40$  °C measured with IR spectroscopy ( $1496\text{ cm}^{-1}$ ). The curve depicts an unweighted least-squares fit to eq 10 that accounts for the shifting dimer–monomer mixtures described by eq 4. A simple fit to  $y = ax^n$  affords  $a = 1.39 \pm 0.05$ ,  $n = 0.57 \pm 0.02$ .

(Figure 6) when fit to a simple power function. The results are consistent with exclusively disolvated-monomer-based metalation (eqs 10 and 11).

$$\frac{d[\text{ArLi}]}{dt} = k[\text{ArH}]^1[\text{S}]^1[\text{A}_2\text{S}_2]^{1/2} \quad (10)$$



**4,4-Dimethyl-2-phenyl-2-oxazoline (4).** The metalation of **4** to form **4-Li** at  $-40$  °C shows a zeroth-order THF dependence (Figure 7). The slight downward drift is too small to be relevant, particularly given subtle secondary-shell effects of similar magnitude;<sup>20</sup> however, there is a subtle and pedagogical reason why it *should* be observable. The THF dependence in conjunction with a half-order LiTMP dependence (Figure 8) are consistent with the monosolvated-monomer-based mechanism (eqs 12 and 13).

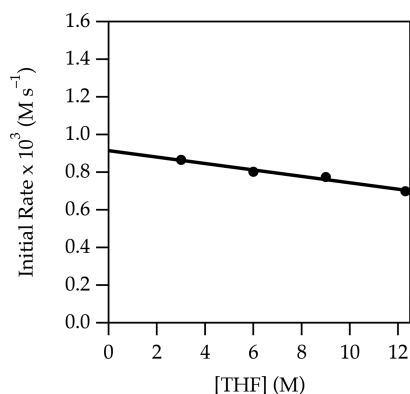


**Figure 7.** Plot of initial rate vs free THF concentration in hexane for the metalation of **4** (0.010 M) at  $-40\text{ }^{\circ}\text{C}$  measured with IR spectroscopy ( $1655\text{ cm}^{-1}$ ). The curve depicts an unweighted least-squares fit to  $y = ax + b$  ( $a = 0.91 \pm 0.02$ ,  $b = -0.017 \pm 0.002$ ).

$$d[\text{ArLi}]/dt = k[\text{ArH}]^1[\text{S}]^0[\text{A}_2\text{S}_2]^{1/2} \quad (12)$$

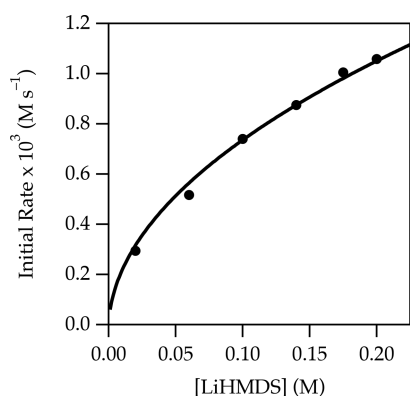
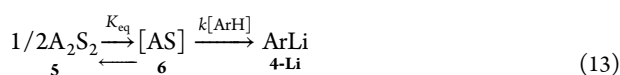


**Figure 8.** Plot of initial rate vs LiTMP concentration in hexane for the metalation of **4** (0.010 M) at  $-40\text{ }^{\circ}\text{C}$  measured with IR spectroscopy ( $1655\text{ cm}^{-1}$ ). The curve depicts an unweighted least-squares fit to eq 12 that accounts for the shifting dimer–monomer mixtures described by eq 4. A simple fit to  $y = ax^n$  affords  $a = 2.7 \pm 0.1$ ,  $n = 0.57 \pm 0.02$ .

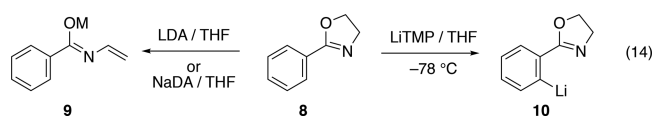
## DISCUSSION

**Qualitative Observations.** The work described herein focuses on rate studies of four LiTMP-mediated orthometalations. It is instructive, however, to qualitatively compare LiTMP with LDA as well as with sodium diisopropylamide (NaDA) based on a survey of approximately 40 arene metalations carried out to choose appropriate substrates for study. Thermochemically recalcitrant metalations such as arene **3** metalate incompletely at equilibrium using excess LDA or NaDA, whereas metalations by excess LiTMP are generally quantitative.<sup>25,26</sup> However, stoichiometric LiTMP also affords an incomplete metalation of **3** at equilibrium, putting the relative thermochemical boost by LiTMP in the vicinity of 1 order of magnitude (a single  $\text{p}K_{\text{A}}$  unit), consistent with the results of Fraser and co-workers.<sup>7</sup> Comparing and contrasting the metalation rates shows that reactions with LiTMP are 5–500 times faster than those with LDA under comparable conditions for the few substrates slow enough to be monitored. By

contrast, metalation rates for LiTMP and NaDA tend to be comparable.<sup>26</sup>

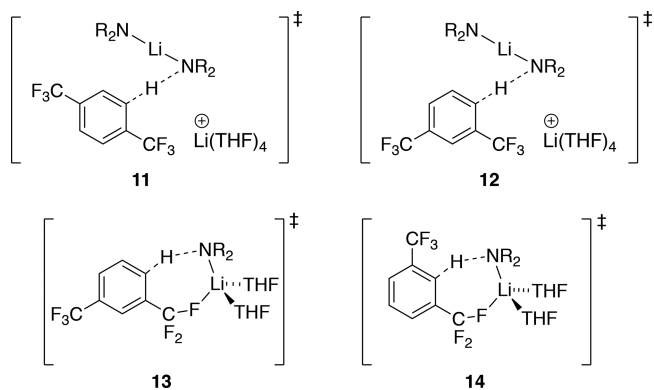
The regioselectivities of LiTMP are distinct from those of either LDA or NaDA. The hindered TMP fragment has two effects: (1) LiTMP metalates less acidic but sterically more accessible sites,<sup>4</sup> such as the 4 position of **2** to give **2-Li**; and (2) the product TMPH does not mediate regiochemical equilibration to the more acidic sites.<sup>10</sup> Previous studies of arene metalations using LDA showed facile equilibration from kinetic to thermodynamic products in the presence of free diisopropylamine: the metalations are reversible.<sup>12</sup> We submit that many reported regioselectivities lack sufficient controls with which to ascertain whether the regioselectivity is the result of kinetic or thermodynamic control.

Contrary to our earlier report,<sup>27</sup> the metalation of **8** lacking the protective gem-dimethyl moiety of **4** by LDA results in decomposition consistent with the formation of **9** rather than the reported orthometalated product **10** (eq 14).<sup>26</sup> Similar



decomposition is obtained with NaDA.<sup>26</sup> By contrast, the LiTMP-mediated ortholithiation of **8** affords **10**, as shown by deuterium quenching, along with limited (15%) decomposition.

**Mechanism of Ortholithiation.** Orthometalation of the four substrates reveals a substrate-dependent mix of mechanisms. Arene **1**,<sup>13a</sup> which has para-disposed  $\text{CF}_3$  moieties, proceeds via a transition structure of stoichiometry  $[\text{A}_2\text{S}_4(\text{ArH})]^\ddagger$ . The high solvation numbers are incompatible with any form of cyclic- or open-dimer-based metalation and instead implicates triple ion **11** analogous to those invoked in a number of previous investigations.<sup>20,22,23</sup> DFT computations suggest a weak dipolar interaction between a fluorine and the lithium cation as evidenced by a minor distortion that does not rise to the level of a discrete contact.



Notably, 1,3-bis(trifluoromethyl)benzene (**2**)<sup>13b</sup> metalates at the external C-4 position with no tendency to equilibrate to the C-2 position. Adding diisopropylamine causes complete equilibration to the 2-lithiated isomer, which confirms that the regioselectivity is under kinetic control. Rate studies reveal a composite of an  $[\text{A}_2\text{S}_4(\text{ArH})]^\ddagger$  dimer-based metalation along with  $[\text{AS}_2(\text{ArH})]^\ddagger$  monomer-based metalation consistent with computed transition structures **12** and **13**, respectively. DFT computations indicate that metalation at C-2 via **14** is a +2.0 kcal/mol higher barrier than that via **13**, consistent with experiment.

1,3-Dimethoxybenzene (**3**) metalates exclusively at the internal (doubly ortho) C-2 position.<sup>13c</sup> Rate studies showed only an  $[\text{AS}_2(\text{ArH})]^\ddagger$  monomer-based pathway. DFT computations revealed a 2.1 Å MeO–Li interaction (15) and affiliated near-tetrahedral lithium coordination sphere (Figure 9).

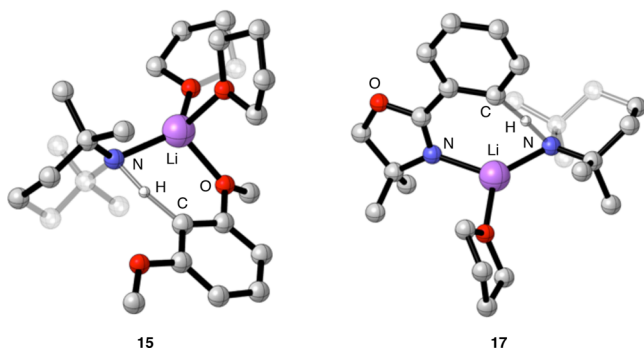


Figure 9. Ball-and-stick representation of transition structures 15 and 17.

Compared with those of 15, computations of the  $\text{AS}_2$ -mediated external metalation (16) also manifested a MeO–Li interaction and a +2.6 kcal/mol higher energy consistent with experiment.

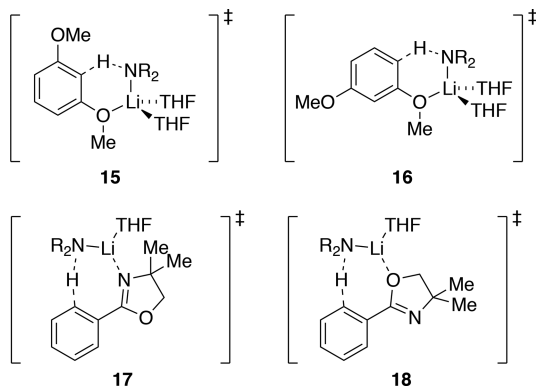


Figure 10. Simulated plot of LiTMP order as a function of percent monomer (measured using normality,  $N$ ). The blue box represents the range accessible to 0.10  $N$  LiTMP in THF/hexane mixtures at  $-78^\circ\text{C}$  (eq 1).



Lithiation of oxazoline **4** proceeds via an  $[\text{AS}(\text{ArH})]^\ddagger$  monosolvated monomer (17).<sup>13d</sup> Previous studies have all supported an N–Li versus O–Li interaction at the transition structure.<sup>28</sup> Indeed, N-bound transition structure 17 (Figure 9) is 4.4 kcal/mol more stable than the O-bound isomer 18. On first inspection, the computed preference along with a seemingly modest 3-fold reduction in metalation rate compared with that of **8** (eq 14) may seem odd given the apparent steric demands of the methyl moieties. However, the methyl moieties in transition structure 17 seem to add no significant congestion.

**Consequence of a Shifting Ground State.** Organolithium mechanistic studies often present the complexity of either mixtures of reactants or multiple competing pathways (rate-limiting transition structures). The latter is a relatively simple kinetic problem of deconvoluting the contributions of a multiterm rate law.<sup>20a</sup> Condition-dependent changes in reactants, by contrast, are far more challenging, historically prompting us to simply avoid them. Only recently did we begin to address the challenges of the influence of multiple reactants on observable rate behavior.<sup>29</sup>

At the outset of the present study, we surmised that a shift in the observable form of LiTMP from purely disolvated dimer (2.0–9.0 M THF/hexane) to a 90/10 mixture of disolvated dimer and disolvated monomer in neat THF (eq 1) would have

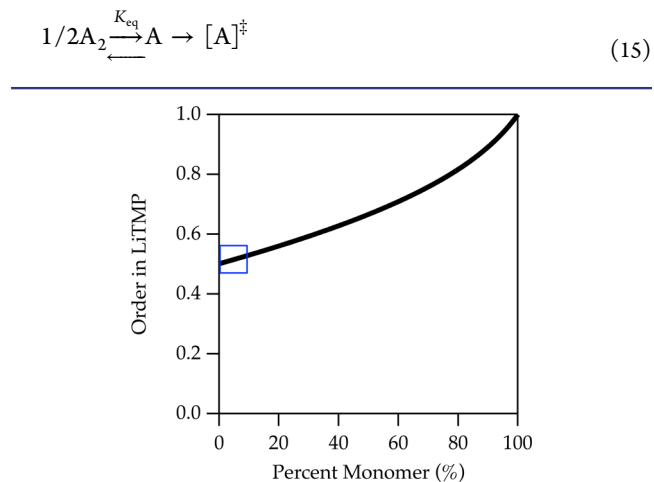
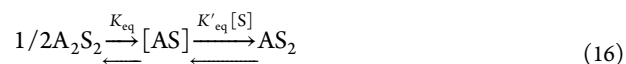


Figure 10. Simulated plot of LiTMP order as a function of percent monomer (measured using normality,  $N$ ). The blue box represents the range accessible to 0.10  $N$  LiTMP in THF/hexane mixtures at  $-78^\circ\text{C}$  (eq 1).

The blue box in Figure 10 shows the dimer–monomer concentration range observed for LiTMP from nearly neat hexane to neat THF. The presence of 10% monomer has an insignificant effect on the measured order ( $n = 0.53$ ). We confess to being a bit surprised. By contrast, owing to the nonlinearity, the perturbation of the measured order when observable monomer is contaminated by 10% dimer is more significant ( $n = 0.82$ ).

This point in the discussion seems to be an opportune time to mention another misunderstood concept about how deaggregation influences reactivity. First, the notion that monomers are more reactive than dimers is by no means a foregone conclusion; this anachronistic thinking derives from rate studies of polymerizations during the 1960s and 1970s.<sup>30</sup> Aggregates often react preferentially.<sup>13c,14,20,23a,31</sup> Second, even if a monomer is the preferred reactive form, changes in solvent or solvent concentration that force monomer formation will not necessarily increase the reaction rate (eq 16). If, for example, “ $\text{AS}$ ” is the reactive form, driving the reactant to  $\text{AS}_2$  by using a high solvent concentration will inhibit the metalation.<sup>29</sup>



## CONCLUSIONS

LiTMP is less nucleophilic than alkylolithiums and more reactive and regioselective than LDA. The absence of amine-mediated equilibration ensures kinetic control of the regioselectivity except when ArH–ArLi direct exchanges are possible.<sup>11</sup> Cost, the primary limitation, appears to be artificial, especially on scales at which competitive pricing should be available. The functional-group-dependent mechanisms,  $[A_2S_4(ArH)]^\ddagger$ ,  $[AS_2(ArH)]^\ddagger$ , and  $[AS(ArH)]^\ddagger$ , determined from a survey of only four substrates representing only two functionalities (MeO and CF<sub>3</sub>) suggest that careful control of conditions, particularly coordinating solvent and solvent concentration,<sup>20a</sup> offers the potential for often overlooked regiocontrol. For the more mechanistically minded, the progress made in addressing mechanisms in which multiple species are observable reactants is notable and remains one of the more serious challenges for exploring complex ensembles.

## EXPERIMENTAL SECTION

**Reagents and Solvents.** THF and *n*-hexane were distilled from solutions containing sodium benzophenone ketyl. LiTMP, [<sup>6</sup>Li]-LiTMP, and [<sup>6</sup>Li,<sup>15</sup>N]LiTMP were prepared as described previously.<sup>16a</sup> Air- and moisture-sensitive materials were manipulated under argon using standard glovebox, vacuum line, and syringe techniques. The arenes were purchased from Sigma-Aldrich.

**NMR Spectroscopy.** All NMR samples for reaction monitoring and structure elucidation were prepared using stock solutions and sealed under partial vacuum as described in detail previously.<sup>9k,20b</sup> Standard <sup>1</sup>H, <sup>6</sup>Li, <sup>13</sup>C, and <sup>15</sup>N NMR spectra were recorded at 500, 73.57, 125.79, and 36.14 MHz, respectively.

**IR Spectroscopy.** IR spectra were recorded using an in situ IR spectrometer fitted with a 30-bounce, silicon-tipped probe. The spectra were acquired in 16 scans at a gain of 1 and a resolution of 4 cm<sup>-1</sup>. A representative reaction was carried out as follows: The IR probe was inserted through a nylon adapter and O-ring seal into an oven-dried, cylindrical flask fitted with a magnetic stir bar and a T-joint. The T-joint was capped with a septum for injections and a nitrogen line. After evacuation under full vacuum, heating, and flushing with nitrogen, the flask was charged with LiTMP (73.6 mg, 0.50 mmol) in THF/hexane (4.9 mL total volume) and cooled to -78 °C with a dry ice/acetone bath. After a background spectrum was recorded, arene **1** was added (0.050 mmol in 0.10 mL) with stirring. The absorbance at 1323 cm<sup>-1</sup> was monitored over the course of the reaction.

## ASSOCIATED CONTENT

### Supporting Information

The Supporting Information is available free of charge on the ACS Publications website at DOI: 10.1021/jacs.8b00590.

Spectroscopic, kinetic, and computational data and authors for ref 19 (PDF)

## AUTHOR INFORMATION

### Corresponding Author

\*dbc6@cornell.edu

### ORCID

David B. Collum: 0000-0001-6065-1655

### Notes

The authors declare no competing financial interest.

## ACKNOWLEDGMENTS

We thank the National Institutes of Health (GM39764) for support.

## REFERENCES

- (1) Murakami, K.; Yamada, S.; Kaneda, T.; Itami, K. *Chem. Rev.* **2017**, *117*, 9302.
- (2) (a) Sartori, G.; Maggi, R. *Chem. Rev.* **2011**, *111*, PR181. (b) Smith, K.; El-Hiti, G. A. *Green Chem.* **2011**, *13*, 1579.
- (3) (a) Yang, Y.; Lan, J.; You, J. *Chem. Rev.* **2017**, *117*, 8787. (b) Shang, R.; Ilies, L.; Nakamura, E. *Chem. Rev.* **2017**, *117*, 9086. (c) Yang, L.; Huang, H. *Chem. Rev.* **2015**, *115*, 3468. (d) Lorion, M. M.; Maindan, K.; Kapdi, A. R.; Ackermann, L. *Chem. Soc. Rev.* **2017**, *46*, 7399.
- (4) (a) Mongin, F.; Quéguiner, G. *Tetrahedron* **2001**, *57*, 5897. (b) Mongin, F.; Quéguiner, G. *Tetrahedron* **2001**, *57*, 4059. (c) Clayden, J. In *The Chemistry of Organolithium Compounds*; Rappoport, Z., Marek, I., Eds.; Wiley: New York, 2004; Vol. 1, p 495. (d) Caubere, P. *Chem. Rev.* **1993**, *93*, 2317. (e) Schlosser, M.; Mongin, F. *Chem. Soc. Rev.* **2007**, *36*, 1161. (f) Hartung, C. G.; Snieckus, V. In *Modern Arene Chemistry*; Astruc, D., Ed.; Wiley-VCH: Weinheim, 2002; Chapter 10. (g) Snieckus, V. *Chem. Rev.* **1990**, *90*, 879.
- (5) (a) Bakker, W. I. I.; Wong, P. L.; Snieckus, V. Lithium Diisopropylamide. In *e-EROS Encyclopedia of Reagents for Organic Synthesis*; Paquette, L. A., Ed.; John Wiley: New York, 2001. (b) Eames, J. Product Subclass 6: Lithium Amides. In *Science of Synthesis*; Snieckus, V., Ed.; Thieme: New York, 2006; Vol. 8a, p 173.
- (6) (a) Campbell, M.; Snieckus, V.; Baxter, E. W. In *e-EROS Encyclopedia of Reagents for Organic Synthesis*; Paquette, L. A., Ed.; John Wiley & Sons: Chichester; New York, 2008; Vol. 5. (b) Mulvey, R. E.; Robertson, S. D. *Angew. Chem., Int. Ed.* **2013**, *52*, 11470.
- (7) Fraser, R. R.; Mansour, T. S. *J. Org. Chem.* **1984**, *49*, 3442.
- (8) Owing to often imprecise usage, we emphasize that driving force connotes exergonicity (thermodynamics).
- (9) (a) Cottet, F.; Schlosser, M. *Eur. J. Org. Chem.* **2004**, *2004*, 3793. (b) Trecourt, F.; Mallet, M.; Marsais, F.; Quéguiner, G. *J. Org. Chem.* **1988**, *53*, 1367. (c) Comins, D. L.; LaMunyon, D. H. *Tetrahedron Lett.* **1988**, *29*, 773. (d) Eaton, P. E.; Cunkle, G. T.; Marchioro, G.; Martin, R. M. *J. Am. Chem. Soc.* **1987**, *109*, 948. (e) Bridges, A. J.; Patt, W. C.; Stickney, T. M. *J. Org. Chem.* **1990**, *55*, 773. (f) Trécourt, F.; Marsais, F.; Güngör, T.; Quéguiner, G. *J. Chem. Soc., Perkin Trans. 1* **1990**, 2409. (g) Gros, P. C.; Fort, Y. *Eur. J. Org. Chem.* **2009**, *2009*, 4199. (h) Cottet, F.; Marull, M.; Lefebvre, O.; Schlosser, M. *Eur. J. Org. Chem.* **2003**, *2003*, 1559. (i) Güngör, T.; Marsais, F.; Quéguiner, G. *J. Organomet. Chem.* **1981**, *215*, 139. (j) Viciu, M. S.; Gupta, L.; Collum, D. B. *J. Am. Chem. Soc.* **2010**, *132*, 6361. (k) Hoepker, A. C.; Gupta, L.; Ma, Y.; Faggini, M. F.; Collum, D. B. *J. Am. Chem. Soc.* **2011**, *133*, 7135. (l) Fukuda, T.; Ohta, T.; Sudo, E.; Iwao, M. *Org. Lett.* **2010**, *12*, 2734.
- (10) (a) Groenendaal, L.; Van Loo, M. E.; Vekemans, J. A. J. M.; Meijer, E. W. *Synth. Commun.* **1995**, *25*, 1589. (b) Plé, N.; Turck, A.; Martin, P.; Barbey, S.; Quéguiner, G. *Tetrahedron Lett.* **1993**, *34*, 1605.
- (11) For discussions of possible slow regiochemical equilibration during an LiTMP-mediated orthometalation, see: (a) Mongin, F.; Desponds, O.; Schlosser, M. *Tetrahedron Lett.* **1996**, *37*, 2767. (b) Schlosser, M.; Marull, M. *Eur. J. Org. Chem.* **2003**, *2003*, 1569. (c) Also, see reference 9l.
- (12) Cantatore, G.; Cassandrini, P. Process for Preparing 2,2,6,6-Tetramethyl-4-Piperdone. U.S. Patent 4,536,581, August 20, 1985.
- (13) Previous orthometalations of substrates 1–4: (a) 1: Capel, V. L.; Dillon, K. B.; Goeta, A. E.; Howard, J. A. K.; Monks, P. K.; Probert, M. R.; Shepherd, H. J.; Zorina, N. V. *Dalton Trans.* **2011**, *40*, 1808. (b) 2: Wang, L.; Wang, Y.; Guo, F.; Zheng, Y.; Bhadury, P. S.; Sun, Z. *Tetrahedron Lett.* **2013**, *54*, 6053. (c) 3: Chadwick, S. T.; Rennels, R. A.; Rutherford, J. L.; Collum, D. B. *J. Am. Chem. Soc.* **2000**, *122*, 8640. (d) 4: Bellamy, E.; Bayh, O.; Hoarau, C.; Trécourt, F.; Quéguiner, G.; Marsais, F. *Chem. Commun.* **2010**, *46*, 7043.
- (14) Wiedemann, S. H.; Ramirez, A.; Collum, D. B. *J. Am. Chem. Soc.* **2003**, *125*, 15893.
- (15) Computations and crystal structures of various MTMP derivatives: Armstrong, D. R.; Graham, D. V.; Kennedy, A. R.; Mulvey, R. E.; O'Hara, C. T. *Chem. - Eur. J.* **2008**, *14*, 8025.

(16) (a) Hall, P. L.; Gilchrist, J. H.; Harrison, A. T.; Fuller, D. J.; Collum, D. B. *J. Am. Chem. Soc.* **1991**, *113*, 9575. (b) Renaud, P.; Fox, M. A. *J. Am. Chem. Soc.* **1988**, *110*, 5702.

(17) Romesberg, F. E.; Collum, D. B. *J. Am. Chem. Soc.* **1992**, *114*, 2112.

(18) (a) Pratt, L. M.; Newman, A.; Cyr, J. S.; Johnson, H.; Miles, B.; Lattier, A.; Austin, E.; Henderson, S.; Hershey, B.; Lin, M.; Balamraju, Y.; Sammonds, L.; Cheramie, J.; Karnes, J.; Hymel, E.; Woodford, B.; Carter, C. *J. Org. Chem.* **2003**, *68*, 6387. (b) Balamraju, Y.; Sharp, C. D.; Gammill, W.; Manuel, N.; Pratt, L. M. *Tetrahedron* **1998**, *54*, 7357.

(19) Frisch, M. J.; Trucks, G. W.; Schlegel, H. B.; Scuseria, G. E.; Robb, M. A.; Cheeseman, J. R.; Zakrzewski, V. G.; Montgomery, J. A., Jr.; Stratmann, R. E.; Burant, J. C.; Dapprich, S.; Millam, J. M.; Daniels, A. D.; Kudin, K. N.; Strain, M. C.; Farkas, O.; Tomasi, J.; Barone, V.; Cossi, M.; Cammi, R.; Mennucci, B.; Pomelli, C.; Adamo, C.; Clifford, S.; Ochterski, J.; Petersson, G. A.; Ayala, P. Y.; Cui, Q.; Morokuma, K.; Malick, D. K.; Rabuck, A. D.; Raghavachari, K.; Foresman, J. B.; Cioslowski, J.; Ortiz, J. V.; Baboul, A. G.; Stefanov, B. B.; Liu, G.; Liashenko, A.; Piskorz, P.; Komaromi, I.; Gomperts, R.; Martin, R. L.; Fox, D. J.; Keith, T.; Al-Laham, M. A.; Peng, C. Y.; Gill, A.; Nanayakkara, C.; Gonzalez, M.; Challacombe, P. M. W.; Johnson, B.; Chen, W.; Wong, M. W.; Andres, J. L.; Gonzalez, C.; Head-Gordon, M.; Replogle, E. S.; Pople, J. A. *Gaussian 09*, Revision A.02; Gaussian, Inc.: Wallingford, CT, 2009.

(20) (a) Collum, D. B.; McNeil, A. J.; Ramírez, A. *Angew. Chem., Int. Ed.* **2007**, *46*, 3002. (b) Algera, R. F.; Gupta, L.; Hoepker, A. C.; Liang, J.; Ma, Y.; Singh, K. J.; Collum, D. B. *J. Org. Chem.* **2017**, *82*, 4513.

(21) We define the idealized rate law as that obtained by rounding the observed reaction orders to the nearest rational order.

(22) Gilchrist, J. H.; Harrison, A. T.; Fuller, D. J.; Collum, D. B.; Romesberg, F. E. *J. Am. Chem. Soc.* **1991**, *113*, 5751.

(23) (a) For attempted compilation of a comprehensive bibliography of triple ions of lithium salts, see: Ma, Y.; Ramírez, A.; Singh, K. J.; Keresztes, I.; Collum, D. B. *J. Am. Chem. Soc.* **2006**, *128*, 15399. (b) Also, see: Reich, H. J. *Chem. Rev.* **2013**, *113*, 7130.

(24) One cannot rigorously exclude a combination of  $[A_2S_3(ArH)]^\ddagger$  and  $[AS_3(ArH)]^\ddagger$ , but both suffer from steric demands associated with the high per-lithium solvation number.

(25) (a) Liang, J.; Hoepker, A. C.; Bruneau, A. M.; Ma, Y.; Gupta, L.; Collum, D. B. *J. Org. Chem.* **2014**, *79*, 11885. (b) Liang, J.; Hoepker, A. C.; Algera, R. F.; Ma, Y.; Collum, D. B. *J. Am. Chem. Soc.* **2015**, *137*, 6292.

(26) Algera, R. F.; Ma, Y.; Collum, D. B. *J. Am. Chem. Soc.* **2017**, *139*, 15197.

(27) Gupta, L.; Hoepker, A. C.; Singh, K. J.; Collum, D. B. *J. Org. Chem.* **2009**, *74*, 2231.

(28) (a) Sammakia, T.; Latham, H. A. *J. Org. Chem.* **1996**, *61*, 1629. (b) Stol, M.; Snelders, D. J. M.; de Pater, J. J. M.; van Klink, G. P. M.; Kooijman, H.; Spek, A. L.; van Koten, F. *Organometallics* **2005**, *24*, 743. (c) Jayasuriya, K.; Alster, J.; Politzer, P. *J. Org. Chem.* **1988**, *53*, 677. (d) Chadwick, S. T.; Ramírez, A.; Gupta, L.; Collum, D. B. *J. Am. Chem. Soc.* **2007**, *129*, 2259.

(29) Reyes-Rodríguez, G. J.; Algera, R. F.; Collum, D. B. *J. Am. Chem. Soc.* **2017**, *139*, 1233.

(30) (a) Hsieh, H. L.; Quirk, R. P. *Anionic Polymerization: Principles and Practical Applications*; Marcel Dekker: New York, 1996. (b) *Ions and Ion Pairs in Organic Reactions*; Szwarc, M., Ed.; Wiley: New York, 1972; Vol. 1 and 2.

(31) (a) Bartlett, P. D.; Goebel, C. V.; Weber, W. P. *J. Am. Chem. Soc.* **1969**, *91*, 7425. (b) Al-Aseer, M. A.; Smith, S. G. *J. Org. Chem.* **1984**, *49*, 2608. and references cited therein. (c) McGarrity, J. F.; Ogle, C. A. *J. Am. Chem. Soc.* **1985**, *107*, 1805. (d) Jones, A. C.; Sanders, A. W.; Bevan, M. J.; Reich, H. J. *J. Am. Chem. Soc.* **2007**, *129*, 3492. (e) Jones, A. C.; Sanders, A. W.; Sikorski, W. H.; Jansen, K. L.; Reich, H. J. *J. Am. Chem. Soc.* **2008**, *130*, 6060.